

See discussions, stats, and author profiles for this publication at: <https://www.researchgate.net/publication/282136010>

Direct and Complete Phosphorus Recovery from Municipal Wastewater Using a Hybrid Microfiltration-Forward Osmosis Membrane Bioreactor Process with Seawater Brine as DS

DATASET · SEPTEMBER 2015

READS

40

4 AUTHORS, INCLUDING:



[Guanglei Qiu](#)

National University of Singapore

33 PUBLICATIONS 394 CITATIONS

[SEE PROFILE](#)



[Subhabrata Das](#)

National University of Singapore

18 PUBLICATIONS 19 CITATIONS

[SEE PROFILE](#)



[Yen-Peng Ting](#)

National University of Singapore

132 PUBLICATIONS 4,312 CITATIONS

[SEE PROFILE](#)

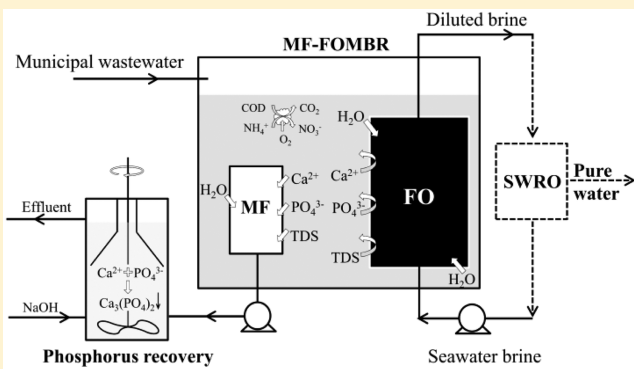
Direct and Complete Phosphorus Recovery from Municipal Wastewater Using a Hybrid Microfiltration-Forward Osmosis Membrane Bioreactor Process with Seawater Brine as Draw Solution

Guanglei Qiu,* Yi-Ming Law, Subhabrata Das, and Yen-Peng Ting*

Department of Chemical and Biomolecular Engineering, National University of Singapore, 4 Engineering Drive 4, Singapore 117585, Singapore

Supporting Information

ABSTRACT: We report a hybrid microfiltration-forward osmosis membrane bioreactor (MF-FOMBR) for direct phosphorus recovery from municipal wastewater in the course of its treatment. In the process, a forward osmosis (FO) membrane and a microfiltration (MF) membrane are operated in parallel in a bioreactor. FO membrane rejects the nutrients (e.g., PO_4^{3-} , Ca^{2+} , Mg^{2+} , etc.) and results in their enrichment in the bioreactor. The nutrients are subsequently extracted via the MF membrane. Phosphorus is then recovered from the nutrients enriched MF permeate via precipitation without addition of an external source of calcium or magnesium. The use of seawater brine as a draw solution (DS) is another novel aspect of the system. The process achieved 90% removal of total organic carbon and 99% removal of NH_4^+-N . 97.9% of phosphate phosphorus ($\text{PO}_4^{3-}-\text{P}$) was rejected by the FO membrane and enriched within the bioreactor. >90% phosphorus recovery was achieved at pH 9.0. The precipitates were predominantly amorphous calcium phosphate with a phosphorus content of 11.1–13.3%. In principle, this process can recover almost all the phosphorus, apart from that assimilated by bacteria for growth. Global evaluation showed an overall phosphorus recovery of 71.7% over 98 days.



INTRODUCTION

Phosphorus is a pollutant but is also an important non-renewable resource. The world phosphorus reserves will run out in a few decades, while its demand continues to rise.¹ One way out of this problem is to recycle phosphorus from various phosphorus-containing waste streams. Municipal wastewater is a hidden treasure for phosphorus, from which 15–20% of the world's phosphorus demand can be satisfied by its recovery.²

Calcium phosphate precipitation is one of the most promising phosphorus recovery processes. Similar to struvite, calcium phosphate is a very important phosphate mineral.¹ Since it is the effective composition of phosphate rocks, it can be more readily accepted by the phosphate industry without limitation.^{3,4} However, the economic application of a phosphorus recovery process usually requires a liquid phase containing high phosphorus content (typically, >50 mg/L^{3,4}), which is not directly suited to municipal wastewater (which typically has phosphorus concentrations of <10 mg/L).² One sensible approach is to use the phosphate-rich side stream or supernatant from digested sludge in wastewater treatment plants with enhanced biological phosphorus removal. However, to produce the phosphate-rich side stream, addition of easily biodegradable organic carbon sources (e.g., acetic acid) is needed to induce the release of phosphate from bacteria.⁵ For the digested sludge supernatant, its high carbonate content

adds to the cost and difficulty in running this process.³ Additionally, before phosphorus reaches the side stream or sludge digestion, it is removed from the wastewater biologically by phosphorus accumulating organisms (PAOs). The cultivation of PAOs requires alternating anaerobic and aerobic/anoxic conditions, adequate amount of organic carbon, and control of the growth of glycogen-accumulating organisms, which restricts the configurations of the wastewater treatment process and affects its reliability.⁶ If phosphorus can be removed and recovered at the very beginning of the wastewater treatment, then significant efforts would be saved in the selection and enrichment of PAOs as well as in the downstream treatment of the phosphorus-rich excess sludge. To date, technologies for direct phosphorus recovery from municipal wastewater are still not available.

Recently, there has been increasing interest in osmotic membrane bioreactor (OMBR) technology due to its advantages in low membrane fouling, the removal of emerging pollutants, and the production of high quality water for reclamation.^{7–9} However, the application of the OMBR is

Received: September 17, 2014

Revised: April 9, 2015

Accepted: April 28, 2015

Published: April 28, 2015

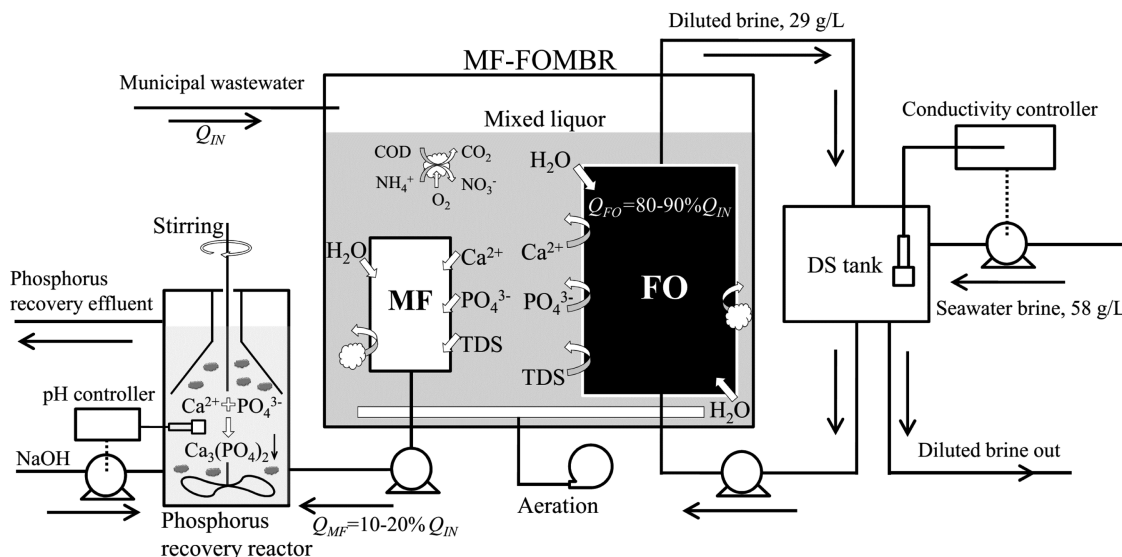


Figure 1. Schematic of the MF-FOMBR phosphorus recovery process.

significantly hampered by salt accumulation which reduces water flux and adversely impacts biological activities.^{10–13} Currently, the control of salt accumulation in the OMBR relies largely on sludge wastage. Increased sludge wastage results in reduced solid retention time (SRT), increased burden of sludge treatment and the loss of slow-growing microorganisms, which significantly limits the OMBR application.^{11,14}

In this study, we demonstrate a hybrid microfiltration-forward osmosis membrane bioreactor (MF-FOMBR) process for direct phosphorus recovery from municipal wastewater in the course of its treatment. In the process, a forward osmosis (FO) membrane and a microfiltration (MF) membrane are operated in parallel in a bioreactor. The FO membrane rejects the nutrients, while the MF membrane allows them to pass through. When water is extracted via the FO membrane, enrichment of the nutrients is achieved in the bioreactor. The nutrients enriched bioreactor supernatant is extracted via the MF membrane. Phosphorus is then recovered from the nutrient-rich MF permeate without the need for addition of calcium or magnesium ions. Aside from the nutrients, other solutes that were rejected by the FO membrane and transported into the bioreactor from the DS can also be extracted via the MF membrane, thus achieving a twin advantage of significantly reducing salt accumulation in the bioreactor.

The use of seawater brine as a draw solution (DS) is another novel aspect of the system. Seawater brine is a waste stream from the seawater reverse osmosis (SWRO) process which requires proper disposal,¹⁵ however it holds high osmotic energy which can be harnessed when the brine is used as a DS.¹⁶ After osmotic dilution, the diluted brine can be returned to the SWRO process without further pretreatment, which would also reduce the operation cost of the SWRO system.^{15,17} Thus, from the resource, material, and energy perspectives, this system is expected to make positive impacts on the environment and the sustainability of wastewater treatment.

MATERIALS AND METHODS

MF-FOMBR Phosphorus Recovery System. A laboratory scale MF-FOMBR phosphorus recovery system was developed to directly harvest phosphorus from municipal wastewater in

the course of its treatment (Figure 1). The system comprises a bioreactor and a phosphorus recovery reactor. The bioreactor (effective volume = 4.50 L) was equipped with an FO module and an MF module (both submerged plate-and-frame modules) operating in parallel. The FO module has two plates. Each plate holds two pieces of cellulose triacetate FO membranes (HTI, Albany, OR) with a total effective membrane area of 0.072 m² and the active layer of the FO membrane facing the activated sludge. Seawater brine collected from Tuaspring Desalination Plant, Singapore (Supporting Information, SI, Table S1) was used as a DS to drive the FO module. To facilitate the evaluation of the FO performance, constant DS concentration (29.0 g/L) was maintained by a conductivity controller (Thermo, Pittsburgh, PA). Seawater brine was pumped into the DS tank whenever the conductivity of the DS dropped below the set point. A peristaltic pump (Cole Palmer, Barrington, U.S.A.) was used to recirculate the DS at 0.2 L/min to minimize external concentration polarization inside the FO plates. The MF module has one plate holding two pieces of polyvinylidene fluoride (PVDF) membranes (Newton and Stokes, Singapore) with the nominal pore size of $\leq 0.1 \mu\text{m}$ and a total effective membrane area of 0.009 m². A peristaltic pump (Cole Palmer, Barrington, U.S.A.) was used to drive the MF module and to get permeate.

A phosphorus recovery reactor was used to receive the MF permeate delivered from the bioreactor for phosphorus recovery. The reactor consisted of a reaction zone (effective volume of 300 mL) and a separation zone (effective volume of 350 mL). The MF permeate was continuously pumped into the reaction zone, where the fluid was continuously stirred at 100 rpm, and constant pH (i.e., 8.5, 9.0, or 9.5) was maintained by a pH controller (Thermo, Pittsburgh, PA) connected to a peristaltic pump (Cole Palmer, Barrington, U.S.A.). 0.2 M NaOH solution was automatically pumped into the reaction zone whenever the pH dropped below the set point. Precipitation of phosphate minerals occurred in the reaction zone under elevated pH. In the separation zone, a funnel-shaped baffle angled at 60° served as a liquid solid separator, which prevented hydraulic mixing above the separator and allowed the solid to settle under gravity. Solids falling onto the separator slid back into the reaction zone. The solids retained

in the reactor were collected at the end of each experimental condition (every 14 days).

The system was operated for 98 days with raw municipal wastewater collected from Ulu Pandan membrane bioreactor (MBR) plant, Singapore (SI Table S2). Activated sludge collected from the same plant was used as the inoculum for the bioreactor. During the operation, the mixed liquor suspended solids (MLSS) concentration was maintained at 4.26–4.52 g/L with an SRT of 50 days.

Two MF flow rates (Q_{MF}) were used (1.0 L/day for Days 1–56 and 2.0 L/day for Days 57–98) to examine the effects on the enrichment of the nutrients, the salt accumulation, the FO performance, and the pollutant removal efficiencies in the bioreactor. Under each Q_{MF} , three reaction pH (8.5, 9.0, and 9.5, with each pH allowed to run for 14 days) were tested in the phosphorus recovery reactor to examine the effects on phosphorus removal and recovery efficiencies and the recovered solid compositions. Detailed operational parameters are provided in SI Table S3.

Analytical Methods. Water samples were collected daily from the influent, the bioreactor, the DS tank, and the effluent of the phosphorus recovery reactor. The chemical oxygen demand (COD), phosphate phosphorus ($PO_4^{3-}-P$), ammonium nitrogen (NH_4^+-N), nitrite nitrogen ($NO_2^- - N$), and nitrate nitrogen ($NO_3^- - N$) were determined according to standard methods.¹⁸ Total organic carbon (TOC) was determined using a TOC analyzer (Shimadzu, Kyoto, Japan). The concentrations of Ca^{2+} , Mg^{2+} , and K^+ were determined using an inductively coupled plasma-optical emission spectrometer (ICP-OES, Thermo, Cambridge, U.K.).

To evaluate the spontaneous precipitation of $PO_4^{3-}-P$ within the bioreactor, 20 mL of mixed liquor was collected from the bioreactor and 0.2 M hydrochloric acid was added to acidify the mixed liquor to pH 4.0. The sample was stirred at 100 rpm for 30 min before the supernatant $PO_4^{3-}-P$, Ca^{2+} , and Mg^{2+} concentration was analyzed.¹⁸ The concentration of the precipitated $PO_4^{3-}-P$, Ca^{2+} , and Mg^{2+} was calculated from the original $PO_4^{3-}-P$, Ca^{2+} , and Mg^{2+} values in the supernatant.

The precipitated solids in phosphorus recovery reactor were collected at the end of each experimental run. After filtering with a 0.45 μm membrane, the solids were air-dried at room temperature before components analysis. Chemical analyses of the recovered solids were performed by dissolving the solids with 10% nitric acid and determining the elemental concentrations in the solutions.¹⁹ Powder X-ray diffraction (XRD) was performed on a diffractometer system (Bruker, Karlsruhe, Germany). The air-dried solids were platinum-coated and observed using a scanning electron microscopy (SEM, JEOL, Tokyo, Japan). Energy dispersive X-ray spectroscopy (EDX) elemental analysis of the solids was performed using a silicon drift detector (INCA, Oxford, U.K.) attached to the SEM.

The particle size distribution of the recovered solids (i.e., those retained in the phosphorus recovery reactor as well as those driven out with the effluent) was determined by a laser granulometer (Beckman Coulter, Brea, CA).

Details of the mass balance evaluation of the enrichment of $PO_4^{3-}-P$, Ca^{2+} , Mg^{2+} , and K^+ in the bioreactor, the global evaluation of phosphorus removal and recovery efficiencies, and modeling of the FO water flux and the salt accumulation in the bioreactor are provided in the SI.

RESULTS AND DISCUSSION

Phosphorus Recovery Alleviates Salinity Build-Up in the Bioreactor. Continuous withdrawal of the bioreactor supernatant through the MF membrane for phosphorus recovery effectively removed the salts that were rejected by the FO membrane and that transported from the DS, thus significantly lowering salinity build-up in the bioreactor (Figure 2). With a MF flow rate (Q_{FM}) of 1.0 L/day, the mixed liquor

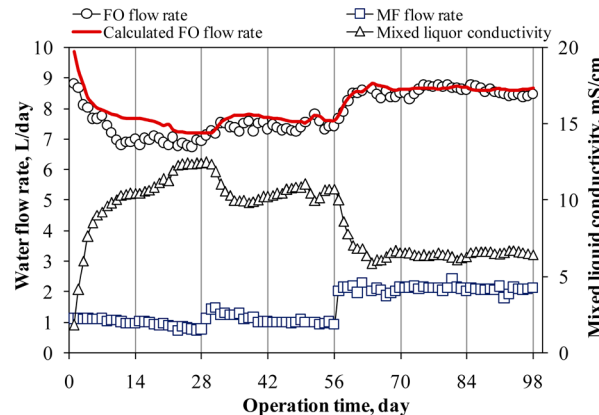


Figure 2. Water flux and salt accumulation patterns in the MF-FOMBR (Day 1–56: MF flow rate (Q_{MF}) = 1.0 L/day; Day 57–98: Q_{MF} = 2.0 L/day). The calculated FO water flow rate is based on the FO water flux calculated according to Loeb et al.³⁹ (SI eq 12).

conductivity stabilized at around 11.5 mS/cm within 10 days. However, a considerable loss in the FO water flux was still observed, reflecting the adverse effect of salinity build-up in lowering the transmembrane osmotic pressure.^{7,8,10} Increase in the Q_{FM} to 2.0 L/day further lowered the mixed liquor salinity to 6.49 mS/cm. FO water flux was also largely restored due to the regaining of the transmembrane osmotic driving force. Although the percentage water recovery decreased from 87.5% to 80.2% (Figure 2), the actual amount of water recovered via FO increased by 24%. Overall, it is evident from the data that the continuous withdrawal of the bioreactor supernatant for phosphorus recovery successfully alleviated salt accumulation in the bioreactor, which resulted in an enhanced treatment capacity of the system.

Enrichment of $PO_4^{3-}-P$, Ca^{2+} , Mg^{2+} , and K^+ in the bioreactor. High rejection of the FO membrane resulted in significant enrichment of $PO_4^{3-}-P$, Ca^{2+} , Mg^{2+} , and K^+ in the bioreactor (Figure 3), which facilitated the subsequent phosphorus recovery by elevating the ionic products and the resultant precipitation potential.³ Confirmed by the mass balance evaluation (SI), $PO_4^{3-}-P$ was effectively concentrated by up to 7-fold with negligible leakage into the DS ($PO_4^{3-}-P < 0.5 \text{ mg/L}$) (Figure 3A). The enrichment of Ca^{2+} , Mg^{2+} , and K^+ in the bioreactor may have resulted from their concentration from the feed wastewater as well as their reverse transport from the DS. Since lower Ca^{2+} , Mg^{2+} and K^+ concentrations were found in the mixed liquor than in the DS (Figure 3B–D), it was manifest that reverse flow into the bioreactor still dominated their bidirectional transport across the FO membrane.^{20,21} Mass balance evaluation (SI) suggested that 12.4%, 38.8%, and 19.7% of the enrichment of Ca^{2+} , Mg^{2+} , and K^+ in the mixed liquor resulted from their reverse transport from the DS. Reverse transport of these ions (especially, Ca^{2+} and Mg^{2+}) not only facilitated phosphorus recovery by providing addi-

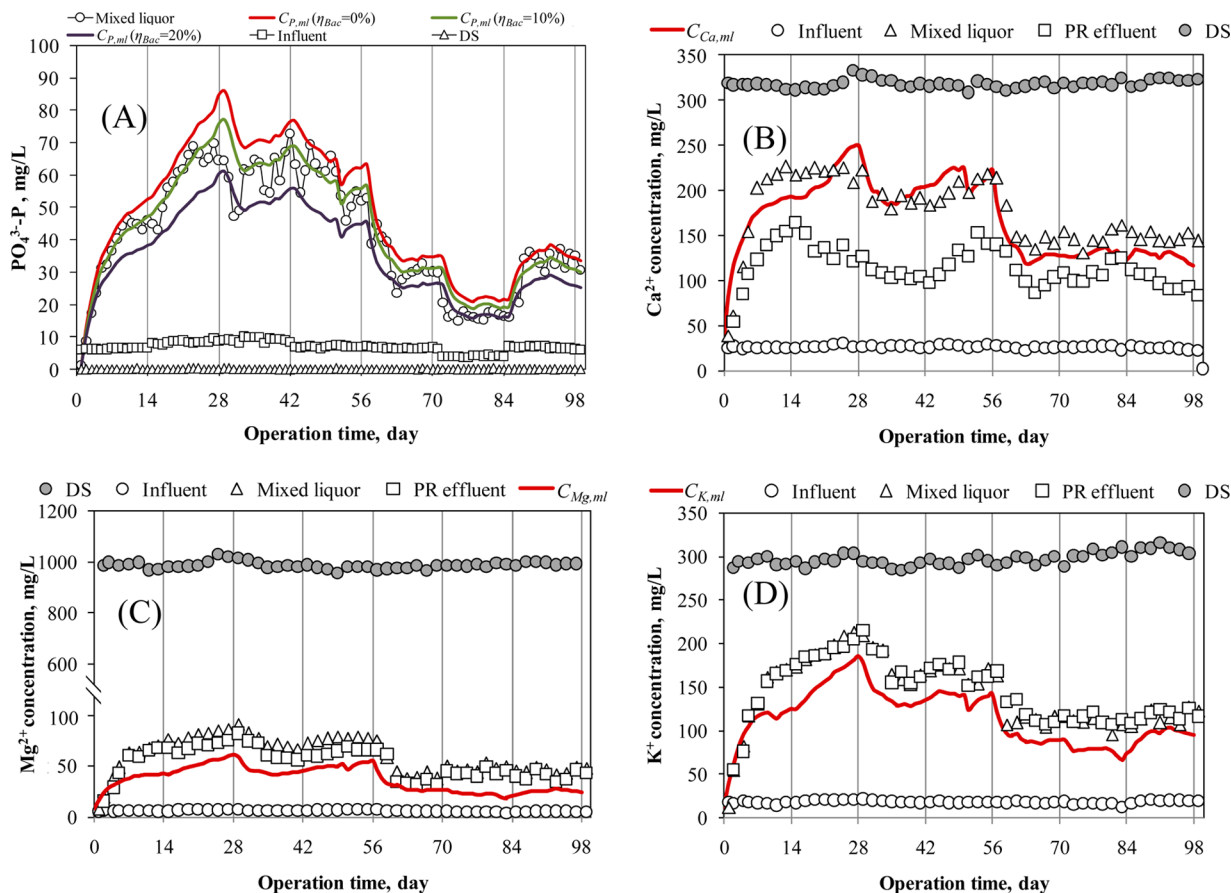


Figure 3. Enrichment of (A) PO_4^{3-} -P, (B) Ca^{2+} , (C) Mg^{2+} , and (D) K^+ in the bioreactor compared with the mass balance calculations. $C_{\text{P},\text{ml}}$, $C_{\text{Ca},\text{ml}}$, $C_{\text{Mg},\text{ml}}$ and $C_{\text{K},\text{ml}}$ are the calculated mixed liquor PO_4^{3-} -P, Ca^{2+} , Mg^{2+} , and K^+ concentration, respectively, based on the mass balance evaluation. η_{Bac} is the assumed percentage of influent PO_4^{3-} -P assimilated by bacteria. (SI eqs 1 and 2).

tional calcium and magnesium source, but also benefited the use of the diluted DS for water production due to reduced scaling potential.²² However, the latter may be negligible since these transported ions only accounted for <1% of their total amount in the DS.

Spontaneous Precipitation of Phosphate Minerals in the Bioreactor. The enrichment of PO_4^{3-} -P, Ca^{2+} , and Mg^{2+} is essential for a subsequent phosphorus recovery. However, too high a concentration may result in their spontaneous precipitation within the bioreactor, thus reducing the amount of dissolved PO_4^{3-} -P that can be extracted via the MF membrane for phosphorus recovery. Indeed, spontaneous precipitation of PO_4^{3-} -P was observed at a Q_{MF} of 1.0 L/day, which resulted in the precipitation of up to 17.7 mg/L PO_4^{3-} -P in the bioreactor due to the formation of calcium phosphates (SI Tables S4 and S5). Increasing Q_{MF} to 2.0 L/day significantly reduced the spontaneous precipitation of PO_4^{3-} -P (SI Table S4) due to the synchronous decrease in PO_4^{3-} -P and Ca^{2+} concentrations and the resultant decrease in the saturation indices (SI) values of calcium phosphates (SI Table S5). This corroborates a study where calcium phosphate precipitation occurred in wastewater treatment systems at sufficiently high concentrations of PO_4^{3-} -P and Ca^{2+} , and redissolution occurred when their concentrations fell below the saturation curve of $\text{Ca}_3(\text{PO}_4)_2$ at neutral pH.²³ Additionally, high PO_4^{3-} -P, Ca^{2+} , and Mg^{2+} concentrations also caused scaling on both the MF and the FO membranes (SI Figure S1), which resulted in a decrease in both the MF and the FO fluxes (Figure 2). The decrease in the MF

flux further aggravated the increase in the mixed liquor PO_4^{3-} -P, Ca^{2+} , and Mg^{2+} concentrations and resulted in an even higher scaling potential. To break from the vicious cycle, new MF and FO membranes were used on Day 28, with a slight increase in the Q_{MF} to reduce the PO_4^{3-} -P, Ca^{2+} , and Mg^{2+} concentrations in the mixed liquor. No remarkable scaling was subsequently observed.

Mixed liquor pH is another key factor which controls the spontaneous precipitation of PO_4^{3-} -P within the bioreactor. During the system operation, the mixed liquor pH was maintained between 5.62 and 6.53, with an average value of 6.18. This pH range is essential in preserving PO_4^{3-} -P in a soluble form within the bioreactor.^{23,24} SI calculation showed undersaturation with all the potential precipitates (except hydroxyapatite ($\text{Ca}_5(\text{PO}_4)_3(\text{OH})$, HAP) at pH = 6.0. However, increase in pH to 6.5 and 7.0 results in a remarkable increase in the SI values of phosphate minerals, which increases the likelihood of their spontaneous precipitation (SI Table S5). Indeed, significant precipitation of phosphate was observed in an anaerobic OMBR when the mixed liquor pH increased from 6.9 to 7.6.²⁵ Therefore, lower pH is desirable in the bioreactor (<6.5). However, low pH inhibits nitrifying activity.²⁶ In this work, a threshold value was observed at around 6.0 below which nitrification was affected (SI Figure S2). Thus, an ideal mixed liquor pH should be within the range of 6.0–6.5.

Phosphorus Removal and Recovery in the Phosphorus Recovery Reactor. In the phosphorus recovery reactor, pH showed distinct effects on the phosphorus removal

efficiencies (Figure 4). For both Q_{MF} (1.0 and 2.0 L/day), there was a notable increase in PO_4^{3-} -P removal when pH was

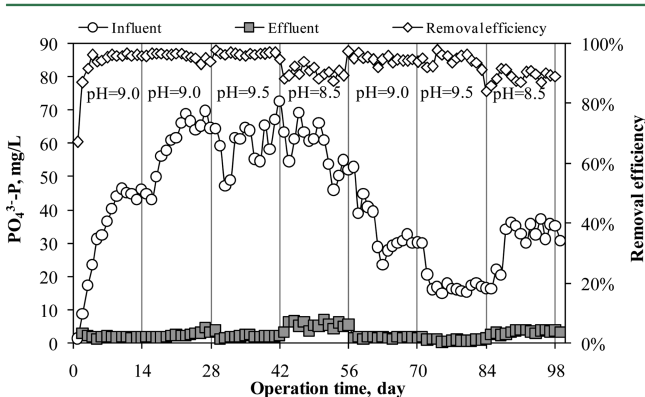


Figure 4. PO_4^{3-} -P removal and recovery in the phosphorus recovery reactor (Day 1–56: MF flow rate (Q_{MF}) = 1.0 L/day; Day 57–98: Q_{MF} = 2.0 L/day).

increased from 8.5 to 9.0. However, further pH increase to 9.5 did not significantly alter the PO_4^{3-} -P removal in a similar fashion. An optimal pH should be around 9.0.

The precipitates were effectively retained (89.9–97.7%) within the phosphorus recovery reactor. However, loss of fine precipitates was still observed as increased amount of solids accumulated within the reactor. Particle size distribution analysis showed lower average particle sizes of the precipitates driven out with the effluent than the solids retained in the reactor (SI Figure S3). Increase in Q_{MF} led to increased loss of fine precipitates, due to the increased upflow velocity (from 0.82 to 1.64 cm/h) in the separation zone. Additionally, shifts in the particle size toward the lower range were noted with increased Q_{MF} , possibly due to the altered hydrodynamics in the reactor under low hydraulic retention time (HRT).²⁷

Removal of Organic Matters and Nitrogen. The system also showed promising results in the removal of organic matters and NH_4^+ -N (SI Figure S2). An initial accumulation of (nondegradable) organic matters was observed within the bioreactor, due to their rejection by the FO membrane.^{13,25} Relatively stable supernatant COD and TOC concentrations were achieved with the continuous withdrawal of the supernatant. Increase in Q_{MF} to 2.0 L/day further reduced the supernatant COD and TOC concentrations to around 50.0 mg/L and 20.0 mg/L, respectively.

With an average influent concentration of 47.7 mg/L, NH_4^+ -N was consistently removed by >99.0%. Compared to

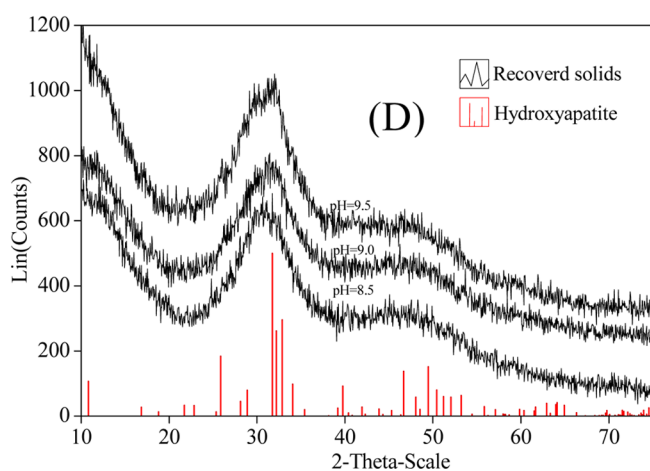
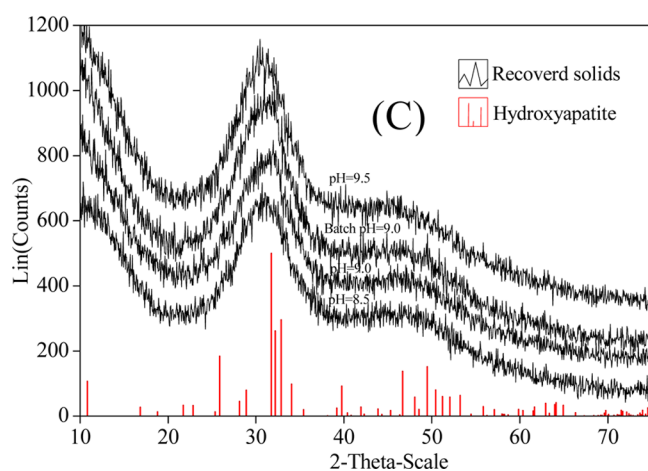
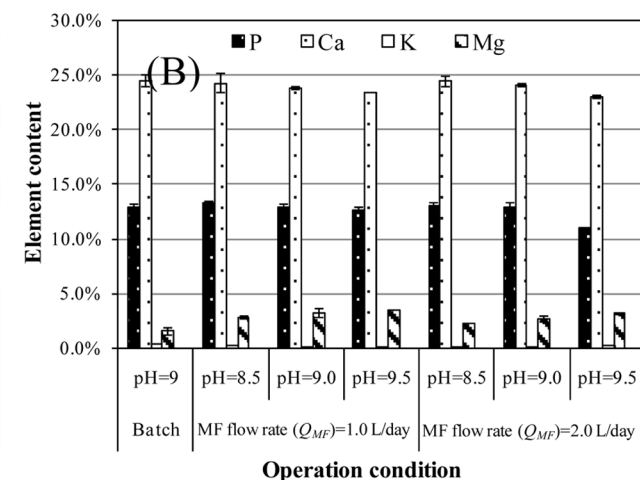
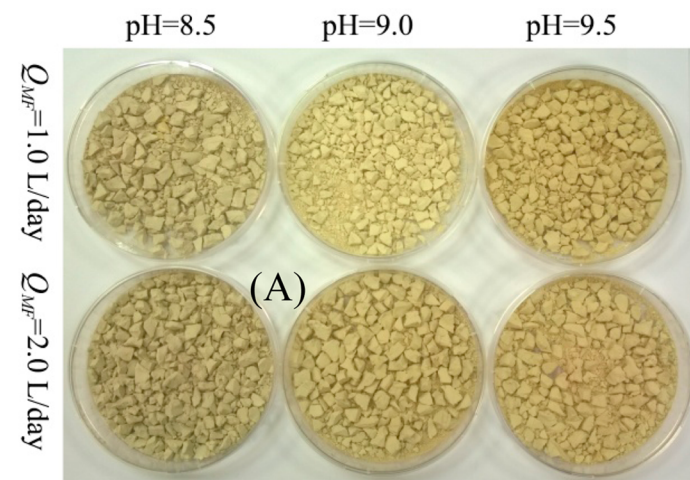


Figure 5. (A) The recovered solids under different conditions, (B) their element contents and XRD diffraction patterns [(C) MF flow rate (Q_{MF}) = 1.0 L/day and (D) Q_{MF} = 2.0 L/day].

previous works,^{13,14} no inhibition of nitrification activities was observed, due to the reduced salt concentration in the bioreactor. However, deterioration in $\text{NH}_4^+ - \text{N}$ removal occurred when the mixed liquor pH dropped below 6.0, due to the limitation in alkalinity²⁶ which resulted in transient $\text{NH}_4^+ - \text{N}$ spikes in the mixed liquor at Days 32 and 65. The steady-state $\text{NO}_3^- - \text{N}$ and $\text{NO}_2^- - \text{N}$ concentrations in the mixed liquor were 4.3–13.3 mg/L and <1.5 mg/L, respectively, suggesting remarkable denitrification although under aerobic conditions. This is considered to be due to the FO membrane rejection of $\text{NO}_3^- - \text{N}$ and $\text{NO}_2^- - \text{N}$, which prolonged their retention in the bioreactor, thus facilitating their aerobic removal.¹³ Phosphorus recovery step did not show substantial removal (<10%) of the organic matters and nitrogen. High rejection of the FO membrane led to minor leakage of TOC and the nitrogen species into the DS (TOC < 5.0 mg/L, $\text{NH}_4^+ - \text{N} < 0.1$ mg/L and average $\text{NO}_3^- - \text{N}$ and $\text{NO}_2^- - \text{N}$ concentration of 2.12 and 0.12 mg/L, respectively), which is favorable for downstream water production.

Recovered Solids. XRD, SEM-EDX, and chemical analyses were used to determine the structure and the composition of the recovered solids (Figure 5). SEM showed loose morphologies of the recovered solids. EDX suggested the predominance of phosphorus and calcium. High carbon content was also detected in the solids, which is due to the deposition/absorption of humic-like substances^{28–31} (SI Figure S4 and Table S6). XRD showed similar diffraction patterns for all the recovered solids, which were predominantly amorphous calcium phosphate (ACP) as indicated by the typical broad peak between the diffraction angles of 25° and 35° (Figure 5C,D).³² Chemical analyses indicated high phosphorus contents in the recovered solids (11.1–13.3%) (Figure 5B). Calcium/phosphorus molar ratio ranged from 1.42–1.60, which is consistent with the theoretical ratio of ACP (1.50). ACP was formed instead of the thermodynamically more stable hydroxyapatite (HAP), possibly due to the slow formation kinetics of HAP,³³ as a result of the latter's higher activation energy for its precipitation over ACP,³¹ and the inhibition effects from Mg^{2+} and humic-like substances.^{30,32} Additionally, the incorporation of magnesium and humic-like substances in the solids, causes local deformation of the crystal structure³⁴ and blockage of the active sites of the newly formed nuclei,^{29,30} which delays HAP nucleation and growth, thus hindering the maturation of ACP into HAP within the phosphorus recovery reactor.

Although reaction pH within the range of 8.5–9.5 did not show substantial impact on the composition of the solids (Figure 5B), a slight decrease in the phosphorus content was observed with the increase in pH due to the incorporation of nonphosphorus-containing minerals (mainly calcium minerals: dolomite, aragonite, calcite. SI Table S5). At the same time, the calcium content decreased while the magnesium content increased due to the increased formation of amorphous magnesium phosphate (AMP) (SI Table S5).³² Additionally, high pH may also have promoted the deposition of humic-like substances, which results in the deepening yellowish-brown coloring of the recovered solids along with the increase in pH (Figure 5A).³⁰

Global Evaluation of Phosphorus Removal and Recovery. A global evaluation was carried out to assess the overall phosphorus removal and recovery efficiencies in the process (SI Table S7). High rejection by the FO membrane led to <2% $\text{PO}_4^{3-} - \text{P}$ loss into the DS, thus ensuring a maximal

amount of $\text{PO}_4^{3-} - \text{P}$ enriched for the subsequent phosphorus recovery. In the phosphorus recovery reactor, $\text{PO}_4^{3-} - \text{P}$ removal decreased with decrease in the reaction pH and increase in Q_{MF} . Overall, 93.2% of $\text{PO}_4^{3-} - \text{P}$ was successfully sequestered in the solids. Taking into account the solids loss with the phosphorus recovery effluent, the phosphorus recovery efficiency was around 90%. By comparing the total amount of phosphorus in the recovered solids with the total influent $\text{PO}_4^{3-} - \text{P}$, the global phosphorus recovery efficiency was shown to be between 56.6% and 83.4% with an overall value of 71.7% over 98 days. The calculated proportion of $\text{PO}_4^{3-} - \text{P}$ that was assimilated by bacteria varied from 2.3% to 21.4%. Taking into account the organic phosphorus present in the influent wastewater, the proportion due to bacteria uptake was considerably stable (between 21.0% and 31.4%, with an overall value of 26.5%). In aerobic activated sludge systems, phosphorus incorporation in the sludge biomass is typically around 0.015 mg/mgMLSS, which results in a phosphorus removal of 15–25% in wastewater treatment plants without enhanced biological phosphorus removal.³⁵ In this work, apart from the bioassimilated portion, almost all the phosphorus was successfully recovered.

Effects of Q_{MF} . Continuous withdrawal of the bioreactor supernatant for phosphorus recovery not only exploits the nutrient-rich supernatant, but also provided a solution to the salt accumulation problem. By increasing Q_{MF} from 1.0 to 2.0 L/day, a few advantages were achieved: (1) Reduced salt concentration in the bioreactor and a resultant enhanced FO flux; (2) Reduced Ca^{2+} , Mg^{2+} , and $\text{PO}_4^{3-} - \text{P}$ concentrations in the mixed liquor and a resultant low spontaneous precipitation potential; and (3) Reduced accumulation of organic matter in the bioreactor and a resultant lower COD concentration in the MF permeate and the phosphorus recovery effluent. Although more fines were driven out with increased Q_{MF} , the overall phosphorus removal and recovery efficiency was not remarkably affected.

Q_{MF} controls the steady-state mixed liquor salt concentration (C_{ml}), the FO water flux, and the steady-state mixed liquor Ca^{2+} , Mg^{2+} , and $\text{PO}_4^{3-} - \text{P}$ concentrations, which is a key parameter in this process. To further illustrate the effects of Q_{MF} , modeling of the steady-state salt concentration, the FO water flux, the percentage water recovery, and the steady-state mixed liquor Ca^{2+} , Mg^{2+} , and $\text{PO}_4^{3-} - \text{P}$ concentrations were obtained and compared with the measured values (SI Figure S5). For the system performance and water recovery, increase in Q_{MF} favors better FO performance by reducing the steady-state mixed liquor salt concentration, but results in decreased percentage water recovery as more water is withdrawn through the MF membrane (SI Figure SSA). For phosphorus recovery, however, although a decrease in Q_{MF} is beneficial since it increases the mixed liquor Ca^{2+} , Mg^{2+} , and $\text{PO}_4^{3-} - \text{P}$ concentrations and the resultant higher precipitation potential, the risk of spontaneous precipitation of ACP is unfortunately also increased within the bioreactor (SI Figure SSB). From both the system performance and the phosphorus recovery point of view, there is an optimal Q_{MF} which, in this work, was around 1.5–2.5 L/day. Generally, the effects of the Q_{MF} ultimately result from the change in the concentration factor (CF) in the bioreactor. For a typical municipal wastewater,^{35,36} an ideal Q_{MF} should be around 1/4–1/6 of the Q_{FO} (i.e., a concentration factor of 5.0–7.0), a value which may be further optimized with respect to different wastewater compositions, DS concentrations and FO membrane performances.

Implications. Phosphorus can be directly recovered by combining a MF membrane within an OMBR, which adds a new advantage to this novel process. The FO membrane rejects phosphorus, thus ensuring a stable and reliable removal. Since no biological activity is required, significant savings can be achieved in obviating the need for the selection and enrichment of PAOs,⁶ as well as the downstream disposal of the phosphorus-rich excess sludge.³⁷ The conflict between phosphorus and nitrogen removal (vis-a-vis the SRT, nitrate inhibition of phosphate release, and the competition on the carbon source) would also be avoided.³⁸ The streamlined phosphorus flow further leads to its high recovery. In principle, almost all the phosphorus can be recovered apart from that utilized by microorganisms. More importantly, the enrichment of Ca^{2+} and Mg^{2+} by the FO membrane eliminates the need for Ca^{2+} and/or Mg^{2+} addition. Nitrification consumes carbonate which further lowers the alkali demand for pH adjustment. The entire scheme may have important implications in current opinions on phosphorus removal and recovery from municipal wastewater. However, $\text{PO}_4^{3-}-\text{P}$ must be in the dissolved form in the bioreactor prior to the phosphorus recovery. To avoid its spontaneous precipitation, low pH (6.0–6.5) is essential.^{23,24} Additionally, since the spontaneous precipitation of $\text{PO}_4^{3-}-\text{P}$ is also governed by the steady-state mixed liquor Ca^{2+} and $\text{PO}_4^{3-}-\text{P}$ concentrations which are dependent on their concentrations in the influent wastewater and the concentration factor of the system, it is important to optimize the concentration factor with respect to specific wastewater Ca^{2+} and $\text{PO}_4^{3-}-\text{P}$ concentrations for a maximal recovery of phosphorus.

Although the OMBR process shows advantages over traditional MBRs, salt accumulation within the bioreactor remains a major challenge.^{10–14} Salinity buildup impacts pollutant removal efficiencies by affecting the biological activities, and lowers the FO water flux by reducing the osmotic drive force. Currently, salt removal in the OMBR relies on the wastage of sludge.^{10–14} Increased sludge wastage results in the decrease in SRT and the loss of slow-growing microorganisms (e.g., nitrifying bacteria).¹⁴ Extensive waste sludge production also increases the burden of subsequent sludge treatment. By combining an MF membrane within an OMBR and continuously withdrawing the bioreactor supernatant for phosphorus recovery, salt accumulation would be controlled within a more manageable range without affecting the SRT. Thus, long SRT may be achieved and maintained, which is essential for the enrichment of slow-growing microorganisms. Sludge production would also be reduced. This salt accumulation control strategy would have important implications in facilitating the practical applications of OMBRs. However, challenges remain to be overcome in the design of FO modules to minimize external concentration polarization and the development of more robust (long lifetime), efficient (high flux and low internal concentration polarization), and selective (low salt leakage) FO membranes for a more cost-effective implementation of the process on a large scale.

Currently, the need of intensive energy input for DS regeneration significantly limits the application of OMBR and other FO related processes. Use of existing and easily accessible high osmotic pressure streams to drive the FO, and a combination with existing concentration processes to regenerate the DS would effectively circumvent this problem. Seawater brine is a waste stream from SWRO,¹⁵ but it is endowed with high osmotic pressure because of the high salt concentration.

The use of seawater brine as a DS exploits the hidden osmotic energy and creates a more sustainable way for its disposal.¹⁶ After osmotic dilution, the diluted brine may be directly discharged to the sea, with reduced impact on the marine ecosystem and environment.¹⁵ Alternatively, it may be returned to the SWRO process as a feed for water production. Substantial savings can be achieved in energy and in the chemically intensive pretreatment.¹⁵ Lower salinity would also reduce the energy consumption in reverse osmosis (RO).¹⁶ However, the efficient reuse of the seawater brine would require the plants to be located nearby. Additionally, the potential accumulation of pollutants and/or membrane foulants in the FO–RO loop in the long term operation remains to be investigated.

ASSOCIATED CONTENT

Supporting Information

Additional experimental details, key properties, and parameters (Tables S1–S7, and Figures S1–S5). The Supporting Information is available free of charge on the ACS Publications website at DOI: 10.1021/es504554f.

AUTHOR INFORMATION

Corresponding Authors

*Tel.: +65 65162190; fax: +65 67791936; E-mail: chetyp@nus.edu.sg (Y.-P.T.).

*Tel.: +65 65162190; fax: +65 67791936; E-mail: cheqg@nus.edu.sg (G.Q.).

Notes

The authors declare no competing financial interest.

ACKNOWLEDGMENTS

This research was funded by the Singapore National Research Foundation under its Competitive Research Program for the project entitled “Advanced FO Membranes and Membrane Systems for Wastewater Treatment, Water Reuse and Seawater Desalination” (grant number: R-279-000-338-281). Special thanks are due to Hydration Technology Inc. for providing the FO membrane material, Ulu Pandan Wastewater Reclamation Plant for providing the municipal wastewater, and Tuaspring Desalination Plant for providing the seawater brine.

REFERENCES

- (1) Hao, X.; Wang, C.; van Loosdrecht, M. C. M.; Hu, Y. Looking beyond struvite for P-recovery. *Environ. Sci. Technol.* **2013**, *47* (10), 4965–4966.
- (2) Yuan, Z.; Pratt, S.; Batstone, D. J. Phosphorus recovery from wastewater through microbial processes. *Curr. Opin. Biotechnol.* **2012**, *23* (6), 878–883.
- (3) Desmidt, E.; Ghyselbrecht, K.; Zhang, Y.; Pinoy, L.; Van der Bruggen, B.; Verstraete, W.; Rabaey, K.; Meesschaert, B. Global phosphorus scarcity and full scale P-recovery techniques: A review. *Crit. Rev. Environ. Sci. Technol.* **2015**, *45*, 336–384.
- (4) Cornel, P.; Schaum, C. Phosphorus recovery from wastewater: needs, techniques and costs. *Water Sci. Technol.* **2009**, *59* (6), 1069–1076.
- (5) Levlin, E.; Hultman, B. Phosphorus recovery from phosphate rich side-stream in wastewater treatment plants. *Proc. Polish-Swedish Semin.* **2003**, *47*–56.
- (6) Oehmen, A.; Lemos, P. C.; Carvalho, G.; Yuan, Z.; Keller, J.; Blackall, L. L.; Reis, M. A.M. Advances in enhanced biological phosphorus removal: From micro to macro scale. *Water Res.* **2007**, *41* (11), 2271–2300.

- (7) Achilli, A.; Cath, T. Y.; Marchand, E. A.; Childress, A. E. The forward osmosis membrane bioreactor: a low fouling alternative to MBR processes. *Desalination* **2009**, *239* (1–3), 10–21.
- (8) Yap, W. J.; Zhang, J.; Lay, W. C. L.; Cao, B.; Fane, A. G.; Liu, Y. State of the art of osmotic membrane bioreactors for water reclamation. *Bioresour. Technol.* **2012**, *122*, 217–222.
- (9) Qiu, G.; Ting, Y. P. Short-term fouling propensity and flux behavior in an osmotic membrane bioreactor for wastewater treatment. *Desalination* **2014**, *332* (1), 91–99.
- (10) Xiao, D.; Tang, C. Y.; Zhang, J.; Lay, W. C. L.; Wang, R.; Fane, A. G. Modeling salt accumulation in osmotic membrane bioreactors: Implications for FO membrane selection and system operation. *J. Membr. Sci.* **2011**, *366* (1–2), 314–324.
- (11) Zhang, J.; Lay, W.; Loong, C.; Chou, S.; Tang, C.; Wang, R.; Fane, A. G. Membrane biofouling and scaling in forward osmosis membrane bioreactor. *J. Membr. Sci.* **2012**, *403*–404, 8–14.
- (12) Lay, W. C. L.; Liu, Y.; Fane, A. G. Impacts of salinity on the performance of high retention membrane bioreactors for water reclamation: A review. *Water Res.* **2010**, *44* (1), 21–40.
- (13) Qiu, G.; Ting, Y. P. Osmotic membrane bioreactor for wastewater treatment and the effect of salt accumulation on system performance and microbial community dynamics. *Bioresour. Technol.* **2013**, *150*, 287–297.
- (14) Wang, X.; Chen, Y.; Yuan, B.; Li, X.; Ren, Y. Impacts of sludge retention time on sludge characteristics and membrane fouling in a submerged osmotic membrane bioreactor. *Bioresour. Technol.* **2014**, *161*, 340–347.
- (15) Elimelech, M.; Phillip, W. A. The future of seawater desalination: Energy, technology, and the environment. *Science* **2011**, *333*, 712–717.
- (16) Song, X.; Liu, Z.; Sun, D. D. Energy recovery from concentrated seawater brine by thin-film nanofiber composite pressure retarded osmosis membranes with high power density. *Energy Environ. Sci.* **2013**, *6*, 1199–1210.
- (17) Hancock, N. T.; Black, N. D.; Cath, T. Y. A comparative life cycle assessment of hybrid osmotic dilution desalination and established seawater desalination and wastewater reclamation processes. *Water Res.* **2012**, *46* (4), 1145–1154.
- (18) APHA. *Standard Methods for the Examination of Water and Wastewater*, 19th ed.; American Public Health Association. Inc.: Washington DC, 1999.
- (19) USEPA. *Test Methods for Evaluating Solid Waste, Physical/Chemical Methods*, SW-8463rd ed. Method 3052; USEPA: Washington, DC, 1995.
- (20) Mallevialle, J.; Odendaal, P. E.; Wiesner, M. R. *Water Treatment Membrane Processes*; McGraw-Hill: New York, 1996.
- (21) Hancock, N. T.; Cath, T. Y. Solute coupled diffusion in osmotically driven membrane processes. *Environ. Sci. Technol.* **2009**, *43* (17), 6769–6775.
- (22) Fritzmann, C.; Löwenberg, J.; Wintgens, T.; Melin, T. State-of-the-art of reverse osmosis desalination. *Desalination* **2007**, *216* (1–3), 1–76.
- (23) Carlsson, H.; Aspegren, H.; Lee, N.; Hilmer, A. Calcium phosphate precipitation in biological phosphorus removal systems. *Water Res.* **1997**, *31* (5), 1047–1055.
- (24) Song, Y.; Hahn, H. H.; Hoffmann, E. Effects of solution conditions on the precipitation of phosphate for recovery: A thermodynamic evaluation. *Chemosphere* **2002**, *48* (10), 1029–1034.
- (25) Chen, L.; Gu, Y.; Cao, C.; Zhang, J.; Ng, J. W.; Tang, C. Performance of a submerged anaerobic membrane bioreactor with forward osmosis membrane for low-strength wastewater treatment. *Water Res.* **2014**, *50*, 114–123.
- (26) Villaverde, S.; García-Encina, P. A.; Fdz-Polanco, F. Influence of pH over nitrifying biofilm activity in submerged biofilters. *Water Res.* **1997**, *31* (5), 1180–1186.
- (27) Pastor, L.; Martí, N.; Bouzas, A.; Seco, A. Sewage sludge management for phosphorus recovery as struvite in EBPR wastewater treatment plants. *Bioresour. Technol.* **2008**, *99* (11), 4817–4824.
- (28) Imai, A.; Fukushima, T.; Matsushige, K.; Kim, Y. H.; Choi, K. Characterization of dissolved organic matter in effluents from wastewater treatment plants. *Water Res.* **2002**, *36* (4), 859–870.
- (29) Cao, X.; Harris, W. G.; Josan, M. S.; Nair, V. D. Inhibition of calcium phosphate precipitation under environmentally-relevant conditions. *Sci. Total Environ.* **2007**, *383* (1–3), 205–215.
- (30) Song, Y.; Hahn, H. H.; Hoffmann, E.; Weidler, P. G. Effect of humic substances on the precipitation of calcium phosphate. *J. Environ. Sci.* **2006**, *18* (5), 852–857.
- (31) Alvarez, R.; Evans, L. A.; Milham, P. J.; Wilson, M. A. Effects of humic material on the precipitation of calcium phosphate. *Geoderma* **2004**, *118* (3–4), 245–260.
- (32) Cao, X.; Harris, W. Carbonate and magnesium interactive effect on calcium phosphate precipitation. *Environ. Sci. Technol.* **2008**, *42* (2), 436–442.
- (33) Nancollas, G. H.; Tomažič, B. Growth of calcium phosphate on hydroxyapatite crystals. Effect of supersaturation and ionic medium. *J. Phys. Chem.* **1974**, *78* (22), 2218–2225.
- (34) Abbona, F.; Baronnet, A. A. XRD and TEM study on the transformation of amorphous calcium phosphate in the presence of magnesium. *J. Cryst. Growth* **1996**, *165* (1–2), 98–105.
- (35) Henze, M.; van Loosdrecht, M. C. M.; Ekama, G. A.; Brdjanovic, D. *Biological Wastewater Treatment: Principles, Modelling and Design*; IWA Publishing: London, 2008.
- (36) Metcalf, L.; Eddy, H. P.; Tchobanoglou, G. *Wastewater Engineering: Treatment, Disposal, and Reuse*; McGraw-Hill: New York, 2004.
- (37) Li, X.; Chen, H.; Hu, L.; Yu, L.; Chen, Y.; Gu, G. Pilot-scale waste activated sludge alkaline fermentation, fermentation liquid separation, and application of fermentation liquid to improve biological nutrient removal. *Environ. Sci. Technol.* **2011**, *45* (5), 1834–1839.
- (38) Chen, Y.; Peng, C.; Wang, J.; Ye, L.; Zhang, L.; Peng, Y. Effect of nitrate recycling ratio on simultaneous biological nutrient removal in a novel anaerobic/anoxic/oxic (A_2/O)-biological aerated filter (BAF) system. *Bioresour. Technol.* **2011**, *102* (10), 5722–5727.
- (39) Loeb, S.; Titelman, L.; Korngold, E.; Freiman, J. Effect of porous support fabric on osmosis through a Loeb–Sourirajan type asymmetric membrane. *J. Membr. Sci.* **1997**, *129* (2), 243–249.